Supporting Information

Efficient and Stable Inorganic Perovskite Solar Cells Enabled by Lead Silicate Glass Layer

Wanpeng Yang[a], Haixuan Yu[a], Zhiguo Zhang[a], Haodan Shi[a], Yong Hu[a], Junyi Huang[a], Zhirong Liu[a], Yan Shen[a,*] and Mingkui Wang[a,b*]

[a] Wuhan National Laboratory for Optoelectronics, Huazhong University of Science and Technology, Wuhan 430074, P. R. China

[b] Optics Valley Laboratory, Wuhan, Hubei 430074, P.R. China

* Corresponding author: E-mail: ciac_sheny@mail.hust.edu.cn, mingkui.wang@mail.hust.edu.cn

Experimental Section

***Materials*:** CsI (99.9%, Sigma-Aldrich), PbI_2 (99.9%, Sigma Aldrich), DMAI (99.9%, Xi'an Polymer Light Technology Corp.), N, N-dimethylformamide (DMF, 99.8%, Sigma-Aldrich), dimethylsulfoxide (DMSO, 99.8%, Sigma-Aldrich), and sodium metasilicate (Na_2SiO_3, ≥98.0%, Sinopharm Chemical Reagent Co., Ltd.) were used as received.

***Devices fabrication*:** The FTO substrates underwent a thorough cleaning process involving sequential ultrasonic baths in detergent solution, ethanol, acetone, and deionized water, each for 20 minutes, followed by drying with a nitrogen gun and a 20-minute exposure to UV-ozone for surface treatment. A compact TiO_2 layer with a thickness of 50 nm was deposited onto the pretreated FTO substrates using spray pyrolysis. This involved the application of a solution composed of titanium isopropoxide (trace metals basis, sourced from Aldrich) in ethyl alcohol, which was heated to 450 °C for a duration of 30 minutes to effect deposition. The 0.7 M $CsPbI_3$ precursor solution was prepared by dissolving CsI and PbI_2 with a 1:1.03 molar ratio in DMF/DMSO (17:3, v/v) and stirring for 24 h in a nitrogen glove box. To prepare the modified perovskite precursor solutions, 20 mg of Na_2SiO_3 were dissolved in 1 mL of DMSO under stirring until complete dissolution was achieved. Varying volumes (25, 50, and 75 uL) of this Na_2SiO_3 precursor solution were then introduced into the perovskite precursor solution to attain different doping concentrations of 1, 2, and 3 mg mL^{-1}, respectively. At an ambient relative humidity of around 35%, the $CsPbI_3$ precursor solution was applied to the substrate via a single-

step spin-coating procedure, involving 3000 rpm for 30 s. Subsequently, all perovskite precursor films underwent annealing at 180 °C for a duration of 4 to 5 minutes. Later, the Spiro-OMeTAD solution was spin-coated onto the above γ-$CsPbI_3$ films at 5000 rpm for 30 s. Lastly, an 80 nm gold counter electrode was evaporated under high vacuum conditions to obtain γ-$CsPbI_3$ based devices with active area of 0.06 cm^2.

Preparation of Spiro-OMeTAD Solution: The Spiro-OMeTAD solution was prepared by dissolving Spiro-OMeTAD (90 mg) into chlorobenzene (1 mL), and then adding t-BP (36 μL) and Li-TFSI (22 μL, 520 mg in 1 mL acetonitrile) into above mixture solution to stir over 12 h.

Characterization: The surface morphology for perovskite films was characterized via a field emission SEM, (Regulus 8100, Hitachi). The X-ray diffraction spectrometry pattern was measured using a Shimadzu XRD-6100 diffractometer (CuK radiation). The optical measurements for the perovskite films were investigated by a UV spectrophotometer (MAPADA UV-6100s) working in the ultraviolet-visible-near infrared (UV-Vis-NIR) range. The Current-Voltage measurements were performed using a solar simulator (96000, Newport-Stratfort 150 W) with a simulated AM 1.5 spectrum and power density of 100 mW cm^{-2}. Water contact angles were measured with an optical CA meter (OCA20, Dataphysics) at room temperature. The photocurrent density–voltage (*J–V*) characteristics of PSCs were measured under 1 sun illumination using a programmable Keithley 2400 digital source meter under AM1.5 G simulated sunlight at 100 mW cm-2 (Oriel, model 91192). The intensity of simulated light was precisely calibrated with an NREL-certified KG5- filtered Si photodiode detector. FTIR spectra were measured using an FTIR spectrometer with a diamond ATR (Nicolet iS50R, Thermo Scientific). XPS was measured by ESCALAB 250Xi. PL was measured by a fluorescence spectrophotometer (LabRAM HR800). The Au electrode of devices was deposited using the metal-organic thin film preparation system of model PD-400S (part number: PD20200069). The HR-TEM images were obtained with a high-resolution transmission electron microscope (JEM-2100F, Japan) in high-resolution mode. TRPL decay was conducted using time-resolved luminescence decay with a time-correlated single-photo counting system. A laser beam with an excitation. The Vienna Ab Initio Package (VASP) was employed to perform all the DFT calculations within the generalized gradient approximation (GGA) using the PBE formulation. The projected augmented wave (PAW) potentials were chosen to describe the ionic cores and take valence electrons into account using a plane wave basis set with a kinetic energy cutoff of 450 eV. Partial occupancies of the Kohn-Sham orbitals were allowed using the Gaussian smearing method and a width of 0.05 eV. The electronic energy was considered self-consistent when the energy change was smaller than 10-4 eV. A geometry

optimization was considered convergent when the force change was smaller than 0.05 eV $Å^{-1}$. Grimme's DFT-D3 methodology was used to describe the dispersion interactions. The Brillouin zone integral uses the surfaces structures of 3 × 3 × 1 monkhorst pack *K*-point sampling. Finally, the formation energies with the Na^+ at different locations in perovskite lattice are calculated.

Supplementary Note 1. Formation energy analysis for the transformation of a mole of PbI_2 pairs into $PbSiO_3$

The energy (E) released when a gaseous Pb^{2+} ion and a gaseous I^- ion are brought together from r = ∞ to r = r_0. Herein, r_0 denotes internuclear distance and is assigned as 288 pm. The energy change associated with the formation of an ion pair from an Pb^{2+}(g) ion and a I^-(g) ion is as follows:

$$E = k\frac{Q_1 * Q_2}{r_0} = -1.6\times10^{-18}\ J$$

To calculate the energy change in the formation of a mole of PbI_2 pairs, we need to multiply the energy per ion pair by Avogadro's number (N_A) and number 2 (two Pb-I bonds for one PbI_2):

$$E(PbI_2) = N_A \times E \times 2 = -1926\ kJ/mol$$

When it comes to $PbSiO_3$, r_0 is assigned as 238 pm. To calculate the energy change in the formation of a mole of $PbSiO_3$ pairs, we need to multiply the energy per ion pair by Avogadro's number (N_A) and number 1 (one Pb-O bond for one $PbSiO_3$):

$$E\ (PbSiO3) = NA \times k\frac{Q_1 * Q_2}{r_0} = -2314\ kJ/mol$$

The above discussion is only a rough estimate of the energy change in the formation of PbI_2 and $PbSiO_3$. More negative the value is, more energy is released. In other words, the transform from PbI_2 into $PbSiO_3$ is thermodynamically favored. We also found some supporting data on https://materialsproject.org/, the predicted formation energy of $PbSiO_3$ is -2.575 eV/atom, whose absolute value is much large that that of PbI_2 (-0.921 eV/atom).

PVSK precursor+Na_2SiO_3

Figure S1. The Optical Photograph of $CsPbI_3$ perovskite precursor solution with Na_2SiO_3 after 24 hours of settling.

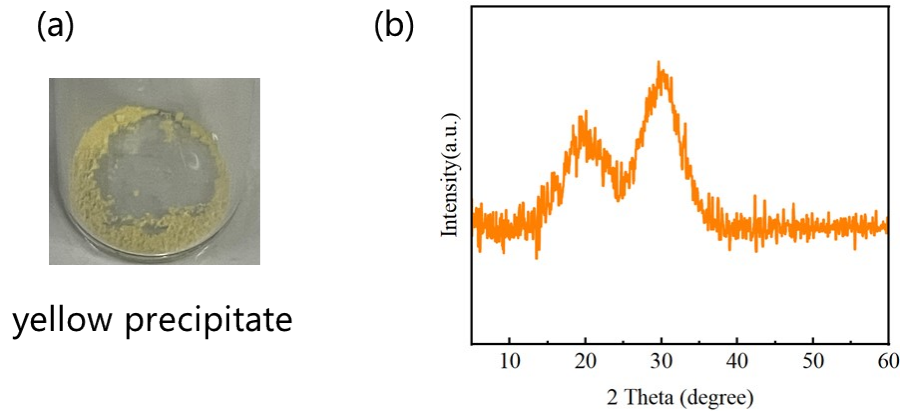

Figure S2. a) Photographs of the yellow precipitations. b) XRD pattern of the yellow precipitation.

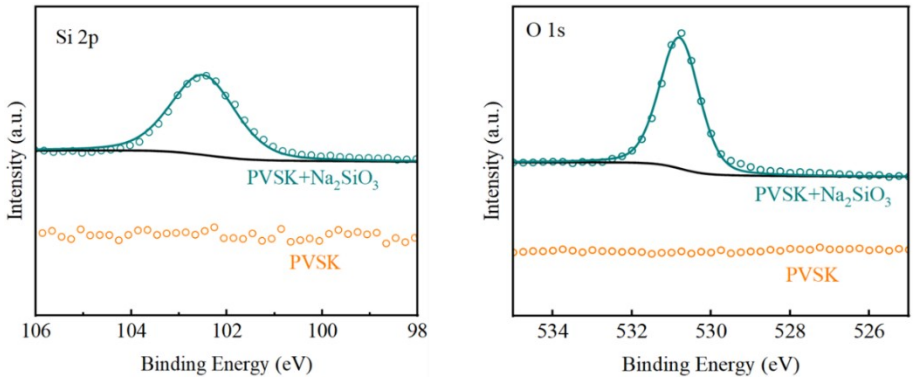

Figure S3. XPS spectra of Si 2p (left) and O 1s (right) species of the $CsPbI_3$ perovskite films with and without Na_2SiO_3 deposited on FTO glass.

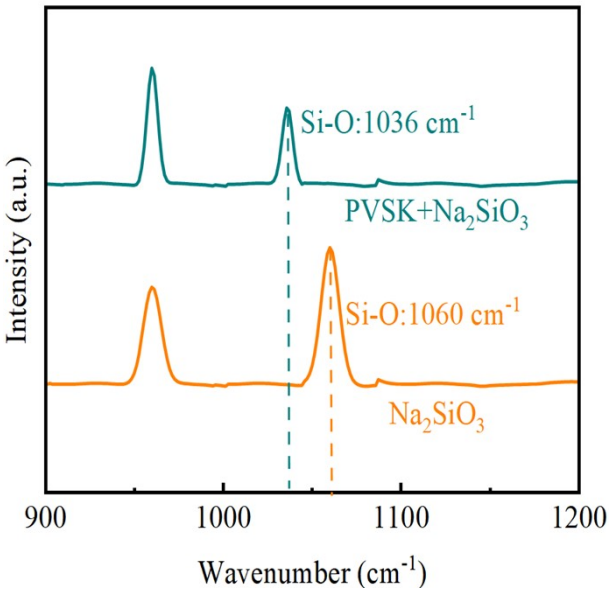

Figure S4. The Raman spectra characterization for the Na_2SiO_3 powder and Na_2SiO_3 modified perovskite film.

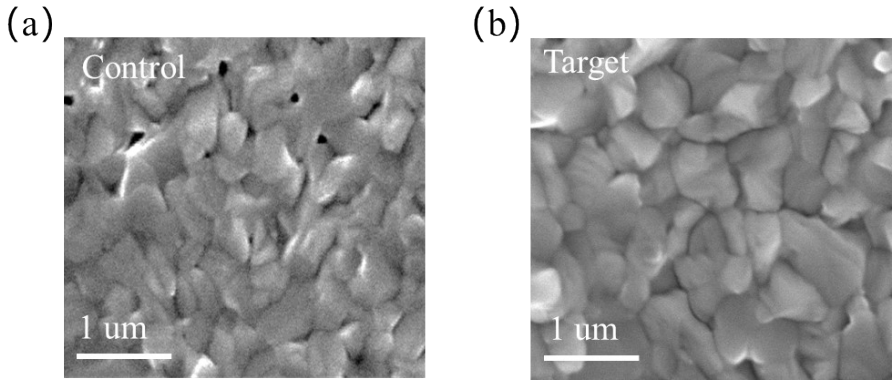

Figure S5. Top-view SEM images of a) control and b) Na_2SiO_3 modified perovskite films.

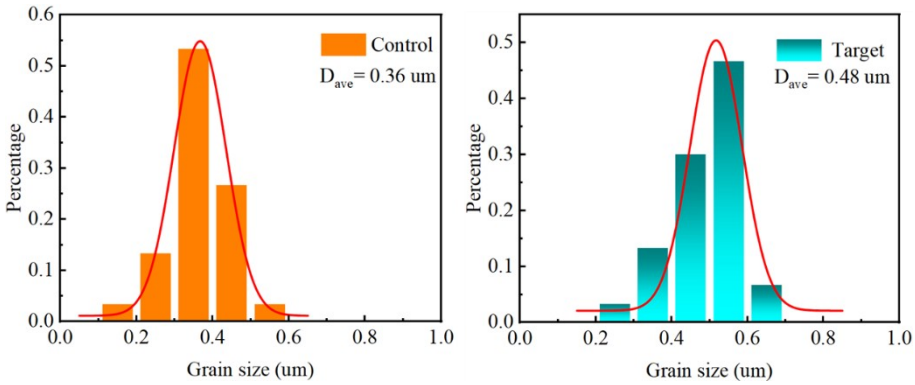

Figure S6. The grain-size statistical distribution of control and target perovskite films.

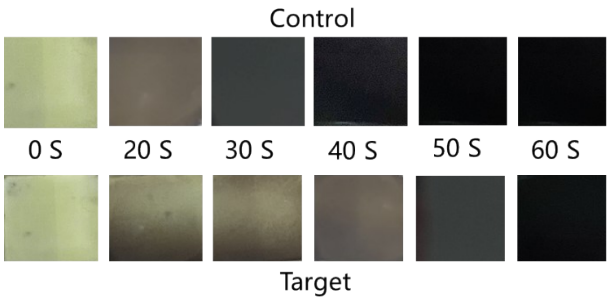

Figure S7. The perovskite films without (upper) and with Na_2SiO_3 (lower) as a function of time under annealing at 180 °C.

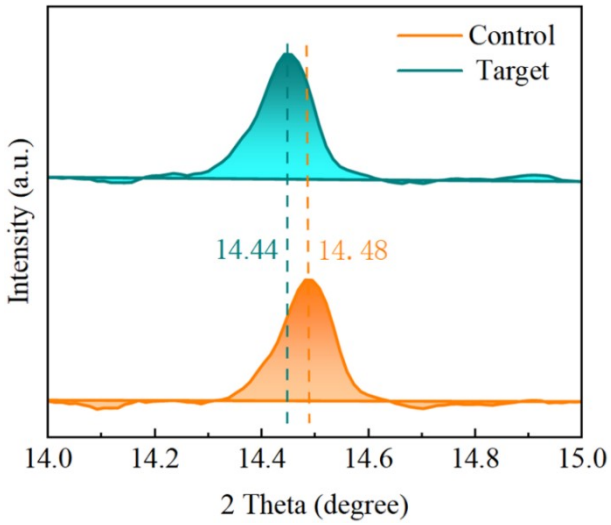

Figure S8. The XRD patterns of control and target perovskite films that local magnification around 2θ =14° to 15°.

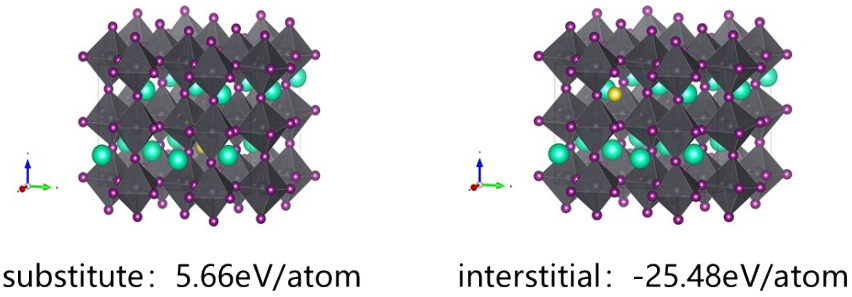

Figure S9. The models of Na ion formation energy at different positions of perovskite.

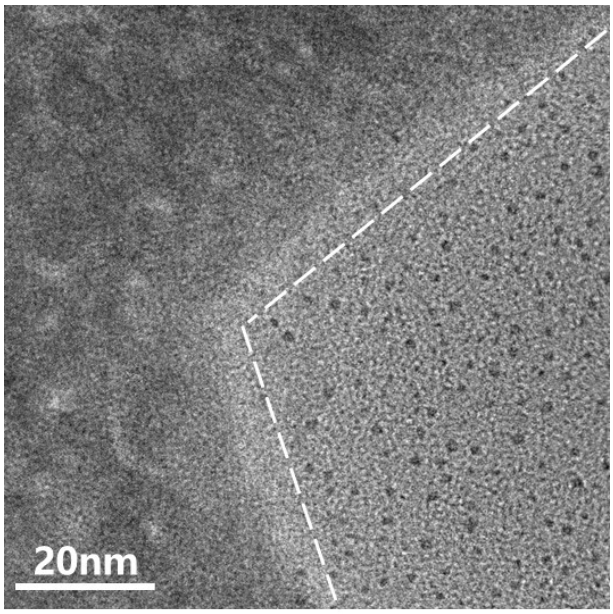

Figure S10. HR-TEM image of the Na_2SiO_3 modified perovskite by ultrasonic dispersion treated the perovskite film in chlorobenzene.

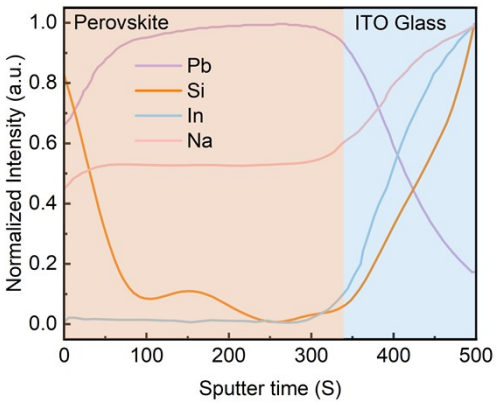

Figure S11. The ToF-SIMS depth profile for Pb, Si, In, and Na elements of $CsPbI_3$ films with high concentration Na_2SiO_3 treated.

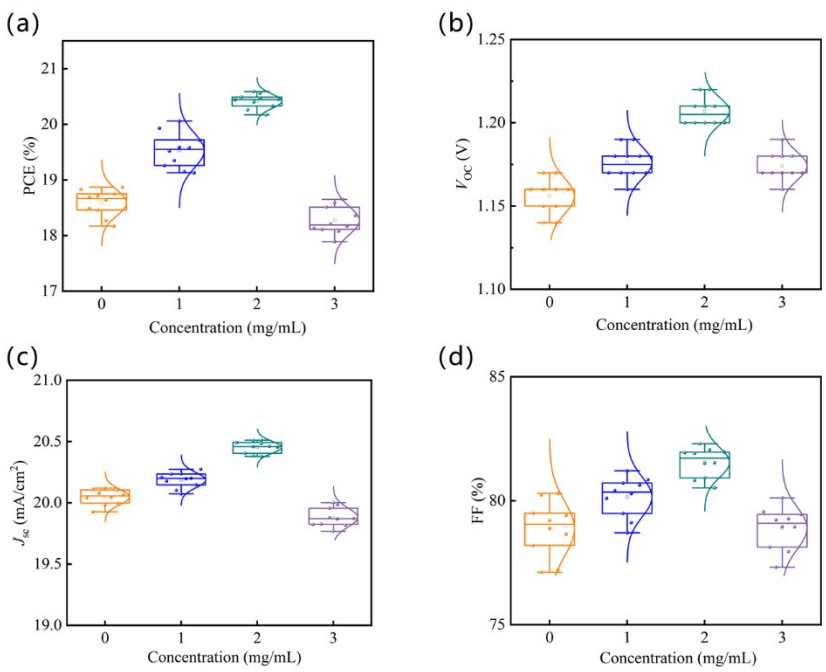

Figure S12. a) The PCE, b) V_{OC} c) J_{SC} and d) FF distribution of PSCs with different concentrations of Na_2SiO_3.

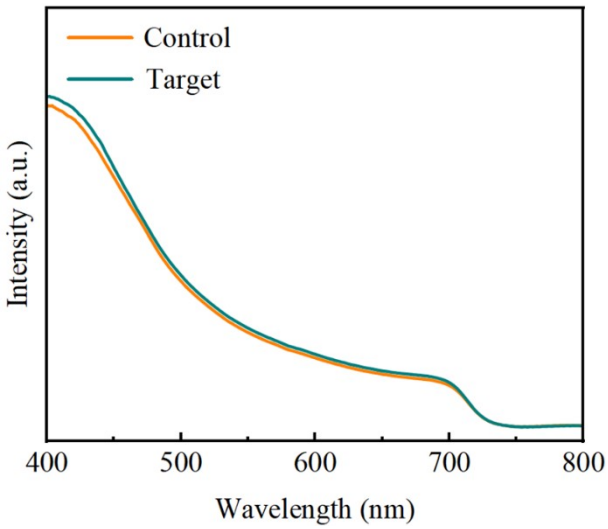

Figure S13. UV–vis absorption spectra of control and target perovskite films.

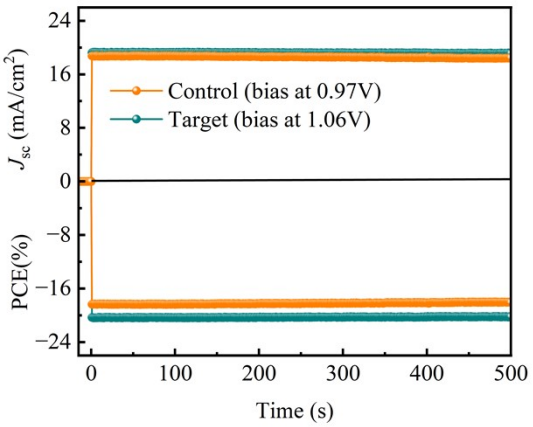

Figure S14. The maximum power point tracking for the control and target devices.

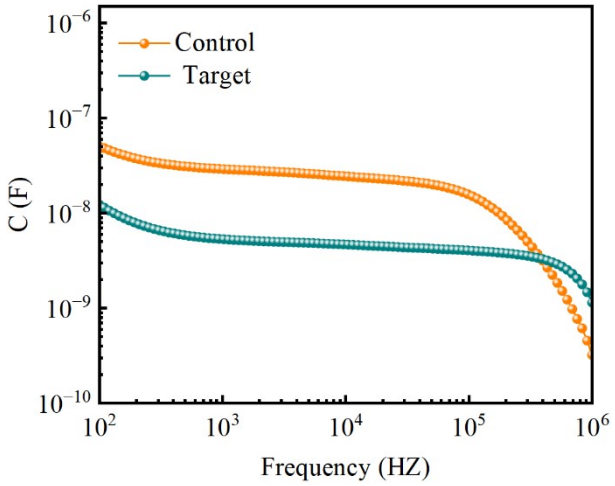

Figure S15. Frequency-capacitance (F-C) measured from control and target PSCs.

According to the following equation:

$$N_T(E_\omega) = -\frac{V_{bi}}{qW}\frac{dC}{d\omega}\frac{\omega}{kT} \quad (1)$$

where C is the capacitance, ω is the angular frequency, k is the Boltzmann constant, and T is the temperature. $E_\omega = E_T - E_V$ where E_T and E_V are the trap energy and valance band maximum, respectively. V_{bi} and W represent the built-in potential and the depletion width, respectively.